

## Equilibrium and kinetic studies on the removal of cadmium(II) by Fe<sub>3</sub>O<sub>4</sub> loaded activated carbon prepared from castor seed shell

Rasappan Vaithianathan<sup>a,\*</sup>, Panneerselvam Anitha<sup>a</sup>, Ramasamy Sudha<sup>b</sup>, Arumugam Ramachandran<sup>a</sup>

<sup>a</sup>Centre for Research, Department of Chemistry, Government College of Engineering, Salem-636 011, Tamil Nadu, India, emails: rvnkishan@gmail.com (R. Vaithianathan), anitha1180@gmail.com (P. Anitha), rams.anbu@gmail.com (A. Ramachandran)

<sup>b</sup>Department of Chemistry, Vivekanandha College of Arts and Sciences for Women (Autonomous), Tiruchengode-637 205, Tamil Nadu, India, email: drsudha@vicas.org

Received 26 March 2023; Accepted 13 July 2023

### ABSTRACT

This study focused to construct a new Fe<sub>3</sub>O<sub>4</sub> magnetic nanoparticles loaded activated carbon (MCSSC) generated from castor seed shell and compare it to raw castor seed shell (CSS) to remove cadmium(II) from wastewater and aqueous solution. The magnetic adsorbent and raw materials are characterized by Fourier-transform infrared spectroscopy, scanning electron microscopy, energy-dispersive X-ray spectroscopy, X-ray diffraction, transmission electron microscopy and Brunauer-Emmett-Teller surface area. The maximum cadmium(II) removal ability of MCSSC and CSS were optimized by various factors of contact time, pH, MCSSC and CSS dose, initial cadmium(II) ion concentrations and temperature using a batch experiment. The maximum monolayer adsorption capacities of cadmium(II) ions onto MCSSC was about 20 times greater than that of CSS and the thermodynamic parameters showed that the exothermic and spontaneous adsorption in nature. The kinetic result demonstrated that followed by pseudo-second-order equation and the rate-limiting step was governed by chemisorption with film diffusion process. The batch experiment with electroplating wastewater and reusability result showed that the MCSSC could be effectively applied for industrial wastewater and exhibited a good reusability up to five cycles as compared to that of CSS.

*Keywords:* Castor seed shell; Cadmium(II); Wastewater; Kinetics; Isotherms

### 1. Introduction

Water is an important natural resource which forms the premise of all life. Water and water resources is very important for maintaining an adequate food supply and productive environment. Due to rapid increasing a population and industrial growth is the major concern for the global demand of fresh water. Water pollution is that the contamination of water bodies, typically as a result of human activities. Water pollution is one of many types of pollution which results from contaminants being introduced into the natural environment [1]. There are many things that can pollute water,

including human waste, agricultural runoff, and industrial effluents. Water pollution may consist of both organic and inorganic pollutants, such as wastes that require oxygen to break down, nutrients from disease-causing plants, sewage, synthetic organic components, and oil. The more prevalent inorganic pollutants, which are linked to industries, roads, and automobiles, are primarily responsible for heavy metal pollution.

The global “load” of hazardous heavy metals in the environment has substantially increased due to industrialization. Cadmium is one of the most widely used metals in a variety of industries including metal processing,

\* Corresponding author.

electroplating, electronics, and a wide range of chemical processing companies [2]. As a result, the presence of cadmium over the allowable levels may result in poisoning and/or organ malfunction, including kidney, liver, brain, reproductive, and central nervous system issues. The Bureau of Indian Standards and World Health Organization states that 0.003 mg·L<sup>-1</sup> of cadmium is the permitted level for drinking water [3,4]. The progress gained in the treatment of cadmium ions in water and wastewater can be acceptable in glow of a rapid description of their sources and toxicity.

Various technologies have been developed to remove heavy metal ions from an aqueous solution, such as ion exchange, membrane process, chemical precipitation, electrochemical treatment, and reverse osmosis [5,6]. Among the above methods adsorption is an extremely efficient and cost-effective method for removing heavy metals from aqueous samples. Many scientists have reported a low cost and high efficiency of adsorbents prepared from several basic and chemically modified natural wastes. However, separating the adsorbents from wastewater is difficult due to their incomplete precipitation. Hence, scientists have explored a magnetic nanoparticle-loaded activated carbon as a suitable method to separate solid particles from the suspension by applying an external magnetic field. This technique has recently gained eminence in the water treatment process and is now recognized as a prospective technique for resolving the above-mentioned issues. However, little work has been done on the preparation of magnetic nanoparticle loaded agricultural waste activated carbon such as prickly pear seed cake [7], mango peel [8], cocoa pod husk [9], oyster shell [10], palm oil shell [11], red mud modified bean-worm skin biochars [12], macromolecular dithiocarbamate/slag-based geopolymer [13], multimetallic silicate adsorbent [14], animal-derived biochar/ferrihydrite composite [15] and mesoporous alginate/ $\beta$ -cyclodextrin polymer [16] are used as adsorbents directly on the application to the extraction of cadmium(II) ions from wastewater.

Castor-oil plant, (*Ricinus communis*), also called castor bean, large plant of the spurge family (Euphorbiaceae), grown commercially for the pharmaceutical and industrial uses of its oil and for use in landscaping. In the current study, castor seed shell, an agricultural waste product that is purchased from the castor seed oil industry, is being used to create a new, inexpensive, and efficient adsorbent.

This study aimed to construct a new Fe<sub>3</sub>O<sub>4</sub> magnetic nanoparticles loaded activated carbon (MCSSC) generated from castor seed shell and compare it to raw castor seed shell (CSS) to purify wastewater and aqueous solution of Cd(II) ions. The magnetic adsorbent and raw materials are characterised by Fourier-transform infrared spectroscopy (FTIR), scanning electron microscopy (SEM), energy-dispersive X-ray spectroscopy (EDX), X-ray diffraction (XRD), transmission electron microscopy (TEM) and Brunauer–Emmett–Teller (BET) surface area. The maximum cadmium(II) removal ability of MCSSC and CSS were optimized by various factors of contact time, pH, MCSSC and CSS dose, initial cadmium(II) ion concentration and temperature. The adsorption ability was estimated by four isotherm models such as Freundlich, Langmuir, Temkin and Dubinin–Radushkevich using non-linear regression analysis by MATLAB R2010b at different temperatures. The adsorption mechanism was

evaluated by various kinetic models. The suitability of the prepared MCSSC was checked by collecting the wastewater sample from the nearby industrial area in Tirupur, Tamil Nadu. The regeneration research also further demonstrates the adsorbent's reusability.

## 2. Materials and methods

### 2.1. Cd(II) solution preparation

The 1,000 mg·L<sup>-1</sup> cadmium(II) solution was arranged by adding 2.282 g of cadmium sulfate in water and diluted to one litre. By dilution of the stock solution with distilled water, 100 mL of cadmium(II) solutions were produced with concentrations of 10–60 mg·L<sup>-1</sup>. These solutions were prepared on the day of use. The 0.1 N HCl or 0.1 N NaOH solutions were taken to alter the solution pH. The nickel-plating industrial effluent was collected from industrial area in Tirupur, India.

### 2.2. Synthesis of raw castor seed shell

Castor seed shell was collected from the local area in Salem district, Tamil Nadu, India. The collected raw material was washed carefully with deionised water to remove dust particles and other impurities. The collected raw materials were dried in a hot air oven at 100°C for 4 h, crushed into powder, and stored in a bottle.

### 2.3. Synthesis of magnetic castor seed shell-based carbon

About 10 g of anhydrous ferric chloride (FeCl<sub>3</sub>) and 5 g of ferrous chloride (FeCl<sub>2</sub>·6H<sub>2</sub>O) was mixed in 200 mL of distilled water and stirred vigorously at 80°C for 30 min. Then 12 g of powered castor seed shell was added, and the solution was stirred for 1 h. Then 20 mL of 25% NaOH solution was added drop wise, and stirring was continued until the black-coloured precipitate was obtained. The precipitate was filtered and dried at 100°C for 12 h. The resultant impregnated samples were activated at 450°C for 3 h in a muffle furnace. After cooling, the activated sample was rinsed with deionized water until the filtrate pH was about 6–7 and dried in a hot air oven for 6 h at 110°C. The obtained samples were named magnetic castor seed shell-based carbon (MCSSC) and stored in a bottle for further experiments.

### 2.4. Batch adsorption experiments

Batch adsorption experiments were carried out in 300 mL plastic bottles containing 100 mL of 10 mg·L<sup>-1</sup> initial metal ion concentration and 0.1 g of adsorbent at pH 7.0. Then the reaction mixture was shaken in a temperature-controlled shaker at a constant speed of 200 rpm at room temperature to change the time for various intervals. The atomic absorption spectroscopy (AAS) was used to determine the amount of heavy metals in the filtrate. Each test was conducted three times, and the reliable results were used for this research. Eqs. (1) and (2) were used to compute the removal effectiveness and amount of cadmium(II) ions adsorbed.

$$\text{Cadmium(II) removal percentage} = \frac{C_i - C_f}{C_i} \times 100 \quad (1)$$

$$\text{Adsorbed efficiency of cadmium(II) ion} = \frac{C_i - C_f}{M} \times V \quad (2)$$

where the adsorbent mass is denoted by  $M$  and is designated as the unit of gram,  $C_i$  and  $C_f$  are the concentration of metal ion at initial and final state in milligrams per liter,  $V$  represent the metal ion solution volume in litre.

### 2.5. Adsorption isotherms

Adsorption isotherms are essential for the development of any adsorption process. At equilibrium, the chemical potential of the solute in the solid phase is identical to that in the liquid phase. The adsorption of cadmium(II) ions at equilibrium onto CSS and MCSSC were correlated by applying the non-linear forms of four different isotherm equations such as Freundlich [17], Langmuir [18], Temkin and Pyzhev [19] and Dubinin–Radushkevich [20] at different temperatures (27°C–47°C) using MATLAB R2010b.

The Freundlich established an empirical relationship between pressure at a specific temperature and the amount of gas absorbed by a unit mass of solid adsorbent. It provides an exponential distribution of active sites and their energies and describes the heterogeneity of adsorbents surface. The non-linearized isotherm equation is expressed as follows:

$$q_e = K_F C_e^{1/n} \quad (3)$$

where  $n$  ( $\text{g}\cdot\text{L}^{-1}$ ) is the degree of non-linearity between adsorption and solution concentration and  $K_F$  is the Freundlich bonding energy constant ( $(\text{mg}\cdot\text{g}^{-1})(\text{L}\cdot\text{mg}^{-1})^{(1/n)}$ ). If  $n > 1$ , adsorption is a physical process; if  $n = 1$  is linear; if  $n < 1$  is a chemical process.

The Langmuir adsorption isotherm model is based on monolayer adsorption onto a homogeneous structure without any reaction between the adsorbed molecules and is represented as follows:

$$q_e = \frac{q_m K_L C_e}{1 + K_L C_e} \quad (4)$$

The maximum monolayer adsorption capacity is  $q_m$  ( $\text{mg}\cdot\text{g}^{-1}$ ), while the Langmuir constant ' $K_L$ ' ( $\text{L}\cdot\text{mg}^{-1}$ ) corresponding to adsorption energy. The dimensionless equilibrium parameter, " $R_L$ ", can be used to measure the attraction between the sorbent and the sorbate by expressing the main properties of the Langmuir isotherm parameters as follows [21]:

$$R_L = \frac{1}{1 + K_L C_0} \quad (5)$$

where  $K_L$  denotes the sorption constant of Langmuir and  $C_0$  is Cd(II) concentration at the initial stage. The Langmuir isotherm's characteristics,  $R_L$ , were discovered to be in the 0 to 1 range implying favourable adsorption.

The Temkin isotherm model considers how the adsorption process is affected by indirect interactions between

the adsorbent and the adsorbate. The following equation is the non-linear form of the Temkin isotherm model:

$$q_e = B \ln(AC_e) \quad (6)$$

In  $B = RT/b$ , the Temkin constant  $b$ , ( $\text{J}\cdot\text{mol}^{-1}$ ) relates to the adsorption of heat and the equilibrium binding constant associated with the highest binding energy is  $A$  ( $\text{L}\cdot\text{mg}^{-1}$ ).

An empirical adsorption model known as the Dubinin–Radushkevich isotherm is frequently used to represent adsorption mechanisms with Gaussian energy distribution onto heterogeneous surfaces [22]. Dubinin–Radushkevich (D-R) model presumes that the adsorbent's surface is heterogeneous and used to fix the type of adsorption process and expressed mathematically by the following equation:

$$q_e = q_{mD} e^{-\beta \varepsilon^2} \quad (7)$$

where  $q_{mD}$  is the D-R monolayer capacity in ( $\text{mg}\cdot\text{g}^{-1}$ ),  $\beta$  is sorption energy constant, and the Polanyi potential ' $\varepsilon$ ' is given as:

$$\varepsilon = RT \ln \left[ 1 + \frac{1}{C_e} \right] \quad (8)$$

where  $T$  denotes the absolute temperature, whereas  $R$  denotes the gas constant of  $8.314 \text{ J}\cdot\text{mol}^{-1}\cdot\text{K}^{-1}$ . The constant  $\beta$  is the activity coefficient, which may be used to compute the mean adsorption free energy  $E$ :

$$E = \left[ \frac{1}{\sqrt{2\beta}} \right] \quad (9)$$

If  $K_{DR} < 8 \text{ kJ}\cdot\text{mol}^{-1}$ , then the sorbate–sorbent interaction directs to physisorption, whereas for  $K_{DR} > 16 \text{ kJ}\cdot\text{mol}^{-1}$ , it predicts as chemisorption [23].

### 2.6. Thermodynamic and kinetic studies

The Effect of temperature tests were carried out using the adsorbents CSS and MCSSC for 100 mL cadmium(II) solution at 10  $\text{mg}\cdot\text{L}^{-1}$  concentrations with an adsorbent doses of 300 (CSS) and 100 (MCSSC) mg at an optimum solution pH and a temperatures of 27°C, 37°C, and 47°C. The mixture was shaken and filtered. The standard entropy ( $\Delta S^\circ$ ), Gibbs free energy ( $\Delta G^\circ$ ) and standard enthalpy ( $\Delta H^\circ$ ) of three thermodynamic parameters were estimated from the experimental data using the Van't Hoff equation is expressed as follows [24]:

$$\Delta G^\circ = -RT \ln K_c \quad (10)$$

$$\ln K_c = \frac{\Delta S^\circ}{R} - \frac{\Delta H^\circ}{RT} \quad (11)$$

where  $K_c = q_e/C_e$  is the equilibrium constant,  $q_e$  and  $C_e$  ( $\text{mg}\cdot\text{L}^{-1}$ ) are the equilibrium adsorption capacities and concentration of metal ions. The  $\Delta S^\circ$  and  $\Delta H^\circ$  values estimated from the intercept and slope of a plot of  $\ln K_c$  vs.  $1/T$ , respectively.

The adsorption kinetics mainly studies the specific process and rate of adsorption of adsorbate on the adsorbent, and the specific adsorption process and rate directly affect the adsorption effect. The various kinetic models, namely, Lagergren's pseudo-first-order, Ho's pseudo-second-order, Elovich, and Weber's intraparticle diffusion, are generally used to identify the dynamics of the adsorption process in order to understand the detailed characteristics of the adsorption process on Cd(II) ions against CSS and MCSSC. In 100 mL of 10–20 mg·L<sup>-1</sup> Cd(II) solution containing the batch kinetic test were conducted for CSS and MCSSC with an optimum pH of 6.0 and adsorbent dose of 100 mg for MCSSC and 300 mg for CSS. The samples were then shaken at a speed of 200 rpm and withdrawn at different time intervals and filtered. The filtrate were analysed by using atomic adsorption spectrophotometer. The amount of metal ion adsorbed at various time periods are calculated by the following equation:

$$q_t = \frac{V}{M}(C_0 - C_e) \quad (12)$$

Lagergren's [25] pseudo-first-order reaction equation was frequently utilised for solid/liquid system adsorption based on solid capacity.

Eq. (13) is the relation between the adsorption amounts at time  $t$  (min),  $q_t$  (mg·g<sup>-1</sup>), and at equilibrium,  $q_e$  (mg·g<sup>-1</sup>) with the rate constant,  $k_1$  (min<sup>-1</sup>) for the pseudo-first-order adsorption.

$$\log(q_e - q_t) = \log q_e - \frac{k_1}{2.303}t \quad (13)$$

A pseudo-second-order model that assumes adsorption follows second-order rate equations [26]. The linear form of the model is shown as follows:

$$\frac{t}{q_t} = \frac{1}{k_2 q_e^2} + \frac{t}{q_e} \quad (14)$$

The Elovich kinetic model is frequently used to interpret adsorption kinetics and effectively describe second-order kinetics when the surface is energetically heterogeneous [27,28]. It is represented by the following equation:

$$q_t = \frac{1}{\beta} \ln(\alpha\beta) + \frac{1}{\beta} \ln t \quad (15)$$

where  $\alpha$  denotes the initial adsorption rate and  $\beta$  represent the desorption constant. The intercept and slope of the plot can be used to calculate Elovich constants by plotting  $\ln t$  vs.  $q_t$ .

### 3. Results and discussion

#### 3.1. Studies on Fourier-transform infrared spectroscopy

FTIR analysis is an essential to investigate the functional groups responsible for the production and confirmation of raw (CSS) and iron oxide-impregnated activated carbon

generated from castor seed shell (MCSSC) adsorbents. The spectrum of the adsorbents was measured between 400 and 4,000 cm<sup>-1</sup> with KBr acting as the background. The FTIR spectra of CSS and MCSSC before and after the adsorption of Cd(II) ions are shown in Fig. 1a and b.

The existence of the Fe–O group is observed in MCSSC around 570–590 cm<sup>-1</sup> [29]. The peak at the O–H stretching vibrations ranges from 3,417 cm<sup>-1</sup> of CSS, has shift to 3,448 cm<sup>-1</sup> in MCSSC which is responsible for the metal-binding process and further shift during cadmium(II) adsorption [30]. The shift in the infrared spectra could be the result of a binding interaction between the metal ion and the carbon atom, which results in the production of metal complexes [31,32]. Furthermore, complexation interactions between metal ions and functional groups on the adsorbent surface were discovered to be the primary driving factor for adsorption mechanisms [33].

The C=O stretching of the –COOH group, represented by the band around 1,745.58 cm<sup>-1</sup> for CSS and MCSSC, respectively [34]. The FTIR spectrum of cadmium(II) ions loaded CSS and MCSSC indicated that the peak values are changed slightly from the original position and their intensity is

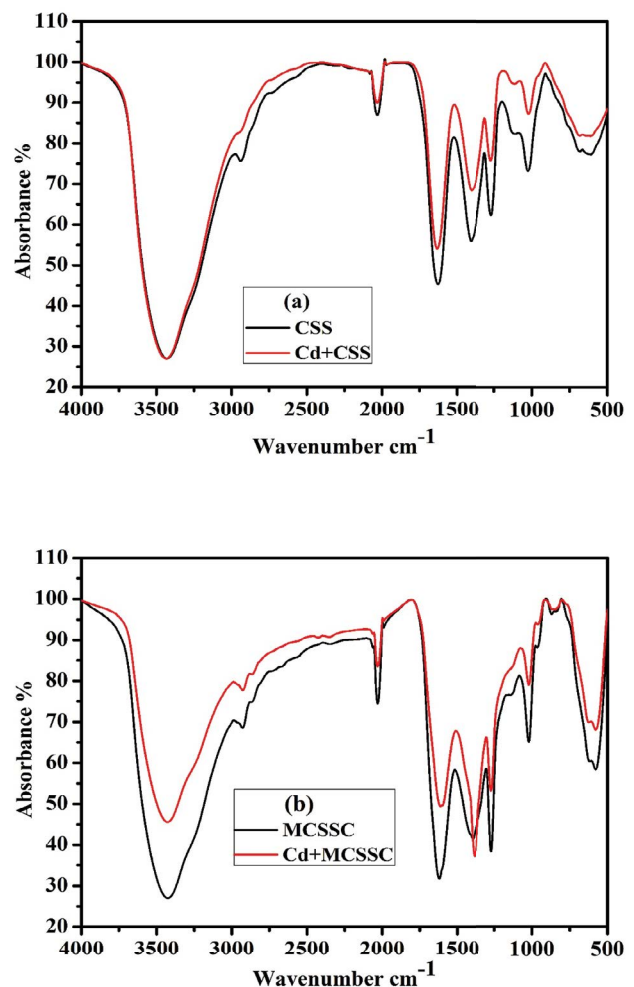


Fig. 1. Fourier-transform infrared spectra of (a) CSS & Cd + CSS and (b) MCSSC & Cd + MCSSC.

shifted. The above observation showed that carboxylic acid and hydroxyl groups in CSS, as well as Fe–O groups that were conformed in MCSSC which is responsible for cadmium(II) extraction from aqueous system.

### 3.2. SEM analysis

Fig. 2a demonstrates that the smooth, uneven, and undulating surface texture of CSS. The vesicles and spaces within this micrograph show no pores, indicating the adsorption capacity of CSS. The CSS was loaded to Fe<sub>3</sub>O<sub>4</sub> and activated during pyrolysis method at high temperatures, which created different pores and cavities on the surface of the carbon designate higher surface area in Fig. 2b. This could be because the pores were occupied with metal ions and other small complex molecules are produced. It is clear that after Cd(II) adsorption, the surfaces and pores of CSS and MCSSC were covered and become smooth by the adsorption of metal ions (Fig. 2c and d).

### 3.3. Studies on EDX image

EDX analysis is a typical analytical method for examining chemical compositions of synthesised CSS and MCSSC. The EDX analysis provides data on the elemental composition of the materials that is both qualitative and quantitative. The EDX spectrum indicates the major elements of calcium, potassium, magnesium ions present in CSS and in addition to that Fe–O group has been introduced to MCSSC during carbonization process followed by co-precipitation method (Fig. 3a and b).

The metal ion uptake was confirmed by the EDX spectrum shown in Fig. 3c and d. The uptake of cadmium(II) ions are evidently revealed in EDX analysis under ion exchange mechanism. This finding suggests that the metal ion peak is increased on the CSS and MCSSC surface and the calcium, potassium, and magnesium peaks are reduced.

### 3.4. XRD, TEM and BET analysis

Fig. 4a shows that the XRD configurations of CSS and MCSSC before and after cadmium(II) adsorption from synthetic effluents, which revealed a slight change in peak position. The well-defined peaks observed in both adsorbents were analysed using XRD analysis, which indicated the crystalline phase of carbon. The crystalline structure of the beads makes them more efficient for cadmium(II) ion adsorption.

The shape and size distribution of the MCSSC were determined using TEM in Fig. 4b. MCSSC is depicted in Fig. 4b as having tiny, compact, monodisperse particles with a mean diameter of 23–27 nm. The dispersion of magnetic particles on the MCSSC surfaces would impact the ease of aqueous ion access to surface active sites of the carbon and to certain pores. As a result, the number of sites accessible for Cd<sup>2+</sup> adsorption, and hence the kinetic and equilibrium behaviour of the adsorption process, are altered.

Fig. 4c depicts their adsorption–desorption isotherms. A highly porous structure and large surface area are necessary for an efficient adsorbent. The magnetic adsorbent's BET surface area, average pore diameter and pore volume were found to be 80.06 m<sup>2</sup>·g<sup>-1</sup>, 3.685 nm and 0.134 cc·g<sup>-1</sup>,

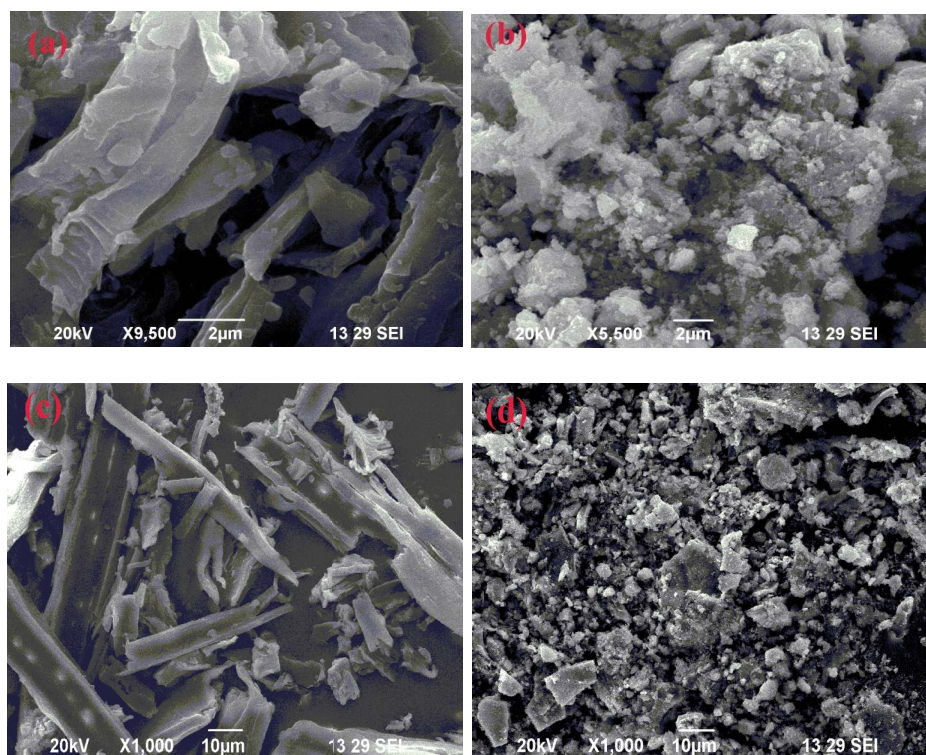


Fig. 2. SEM image of (a) CSS, (b) MCSSC, (c) Cd + CSS and (d) Cd + MCSSC.

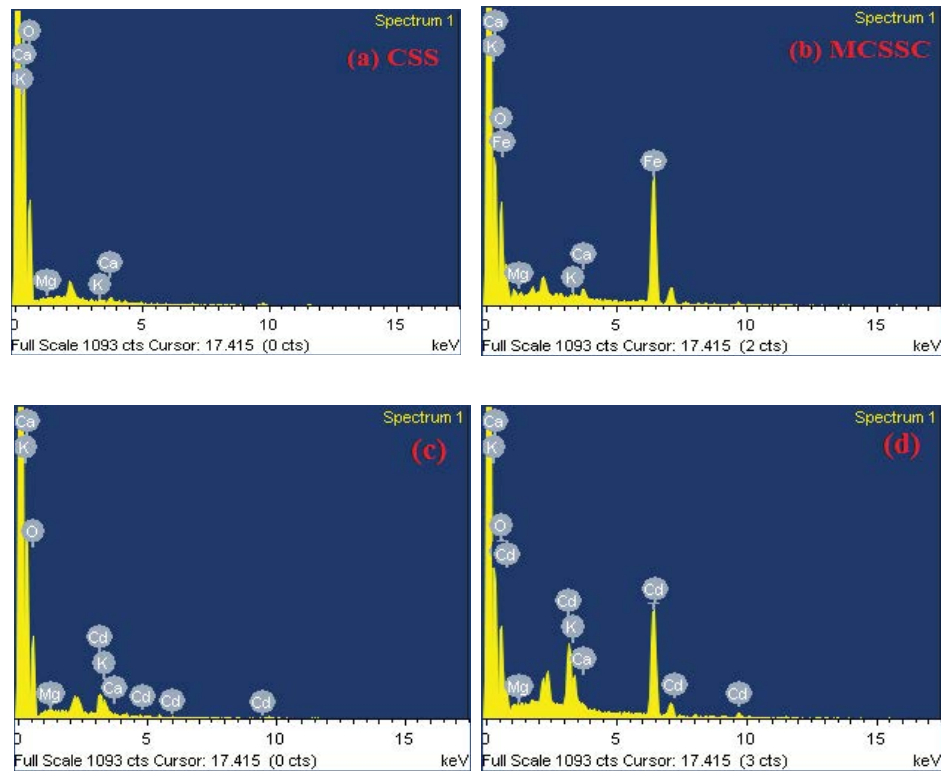


Fig. 3. Energy-dispersive X-ray spectroscopy image of (a) CSS, (b) MCSSC, (c) Cd + CSS and (d) Cd + MCSSC.

respectively. This adsorbent's high surface area is partially due to its microporosity and is more efficient for the adsorption of cadmium(II) ion.

### 3.5. Effect of agitation time on the cadmium(II) elimination efficiency

The agitation period significantly affects the adsorption rate of toxic metal ions. The cadmium(II) removal onto CSS and MCSSC was calculated as a function of varying agitation time (30–180 min) and initial metal ion concentrations ( $10 \text{ mg}\cdot\text{L}^{-1}$ ) using pH 7.0 and constant CSS and MCSSC dose of  $100 \text{ mg}$  are shown in Fig. 5.

Fig. 5 reveals that the sorption efficiency increases rapidly with time and attain equilibrium for 150 min for CSS and 120 min for MCSSC. Further increase in the agitation time does not affect the removal process; that may be due to exhaustion of binding sites in CSS and MCSSC. According to the results, a 120 min equilibrium time was sufficient for the maximum removal of  $94.5\% \pm 0.3\%$  cadmium(II) by MCSSC and  $36.5\% \pm 0.3\%$  removal by CSS. Hence, the optimal contact time was maintained for further experiments such as 150 min for CSS and 120 min for MCSSC, respectively.

### 3.6. Effect of pH on the removal efficiency of cadmium(II) ions

The pH of the solution is a crucial factor that determines the adsorption performance of the adsorbent. The pH value of the aqueous solution affects the metal ion solubility, degree of ionization and counter ions concentration on the

surface of the adsorbent. The effect of pH was investigated by adjusting the initial pH from 2.0–9.0 on the removal of  $100 \text{ mL}$  of  $10 \text{ mg}\cdot\text{L}^{-1}$  cadmium(II) ions onto CSS and MCSSC whereas all other parameters was taken a constant value are given in Fig. 6. The pH effect was determined significantly within the range of 2.0 to 9.0 to avoid the metal ions precipitation at higher pH. It could be seen from Fig. 6 that the percentage removal of cadmium(II) ions was increased by increasing the solution pH from 2.0 to 6.0 and decreases after a pH of 7.0. It can be seen that at a pH of around 6.0, cadmium(II) ions were removed at a greater rate of  $99.2\% \pm 0.4\%$  for MCSSC and in the case of CSS was  $47\% \pm 0.4\%$  only. It is clear that the decreasing rate of cadmium(II) ions was significantly reduced under alkaline conditions.

Cd(II) adsorption of CSS and MCSSC increased rapidly at the initial pH 2.5–4.0, then gradually stabilized at higher pH 4.0–7.0. The surface functional groups of CSS and MCSSC were protonated at lower pH and deprotonated at higher pH. At lower initial pH 2.0–3.0, the surface of CSS and MCSSC were protonated, and the reduction of electrostatic attraction made the active sites less available for cadmium(II) adsorption. Meanwhile, the competition of  $\text{H}^+$  cations further leads to reduction of adsorption. In the initial pH 4.0–7.0, the increase of pH facilitated the degree of dissociation of acidic functional groups on the carbon's surfaces, thus enhancing Cd(II) adsorption via electrostatic attraction, and hence the electrostatic interactions between the functional groups and Cd(II). Hence, the optimal pH was maintained for further experiments at 6.0 for CSS and MCSSC, respectively.

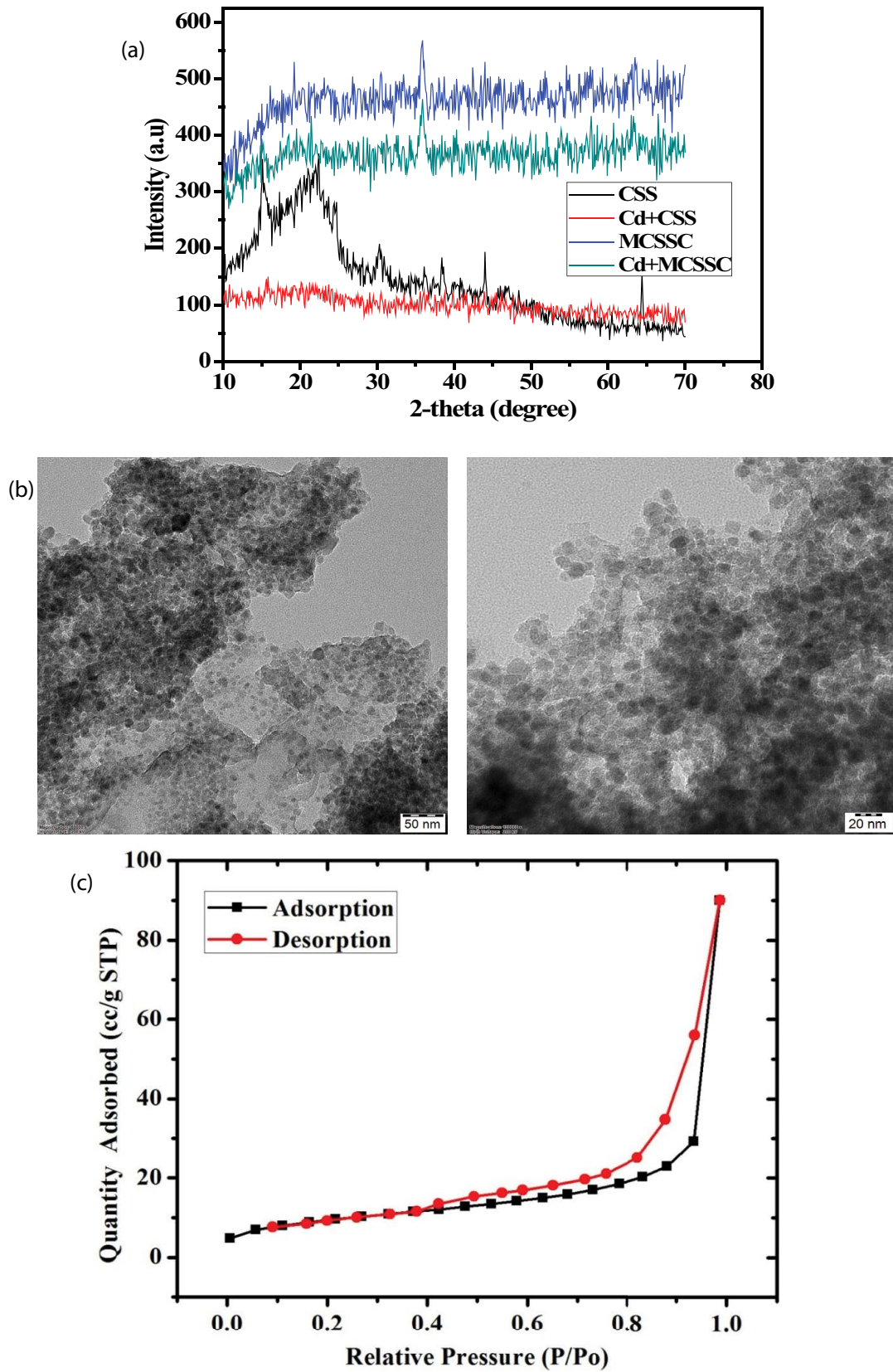


Fig. 4. (a) X-ray diffraction study for CSS and MCSSC before and after the adsorption of Cd(II) ions. (b) Transmission electron microscopy image for synthesised MCSSC from castor seed shell. (c) Nitrogen adsorption–desorption isotherm for synthesised MCSSC.

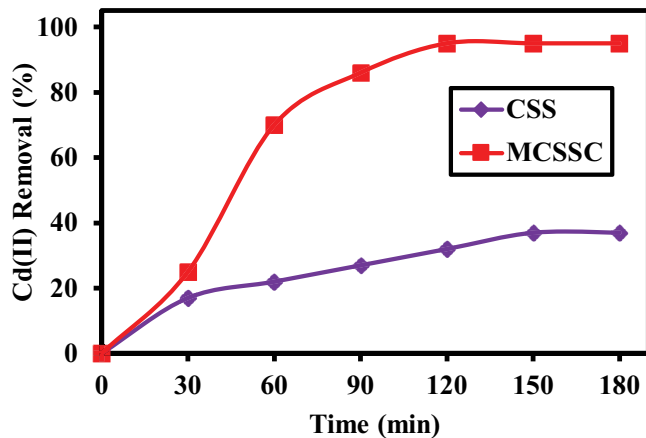


Fig. 5. Influence of agitation time for cadmium(II) elimination onto CSS and MCSSC (Cd(II) concentration  $10 \text{ mg}\cdot\text{L}^{-1}$ ; adsorbent dose  $100 \text{ mg}$  and  $\text{pH}$  7).

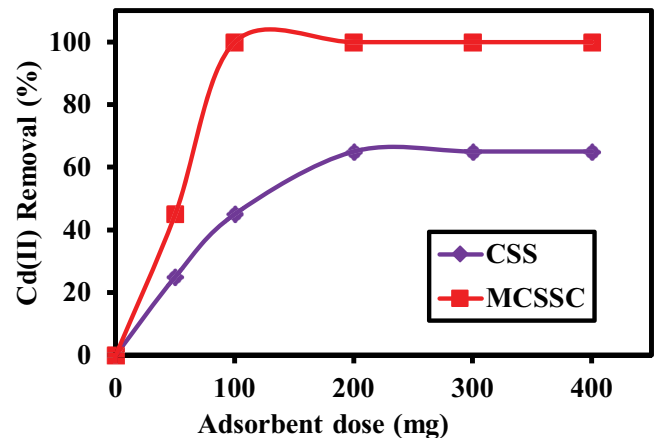


Fig. 7. Effect of CSS and MCSSC dose for the removal of Cd(II) (Cd(II) concentration  $10 \text{ mg}\cdot\text{L}^{-1}$ ;  $\text{pH}$  6.0; contact time 120 min for MCSSC and 150 min for CSS).

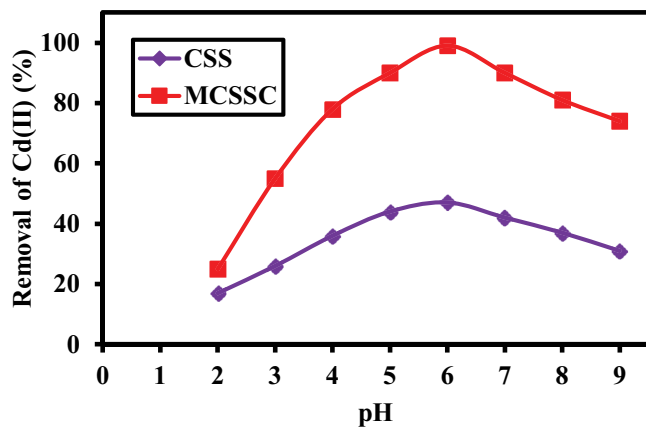


Fig. 6. Effect of  $\text{pH}$  for Cd(II) removal onto CSS and MCSSC (Cd(II) concentration  $10 \text{ mg}\cdot\text{L}^{-1}$ ; adsorbent dose  $100 \text{ mg}$  and contact time 120 min for MCSSC and 150 min for CSS).

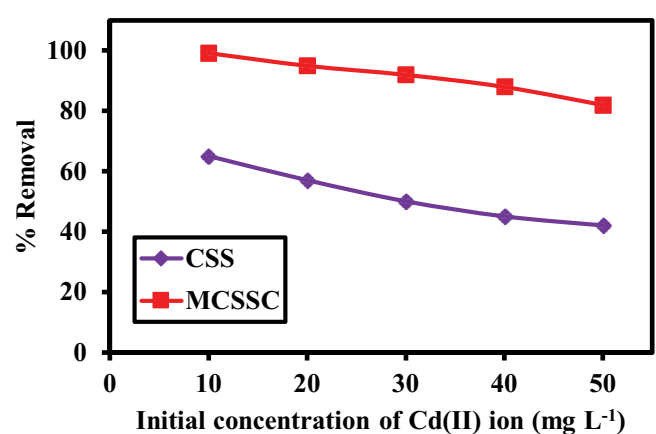


Fig. 8. Effect of Cd(II) ion concentration onto CSS and MCSSC ( $\text{pH}$  6.0; contact time 120 min for MCSSC and 150 min for CSS; MCSSC dose  $100 \text{ mg}$  and CSS dose  $300 \text{ mg}$ ).

### 3.7. Effect of CSS and MCSSC dose on the removal of Cd(II)

The adsorbent dose is a vital parameter for determining the adsorbent's adsorption capacity for removing polluted ions from the wastewater. In order to find out the minimum amount of CSS and MCSSC required for the maximum removal of Cd(II), experiments were conducted using  $10 \text{ mg}\cdot\text{L}^{-1}$  of Cd(II) solutions with varying amounts of adsorbent dose ranging from  $50\text{--}400 \text{ mg}/100 \text{ mL}$  at an optimum  $\text{pH}$  of 6.0 and agitation time of 120 min for MCSSC and 150 min for CSS are given in Fig. 7. From Fig. 7 it can be seen that a minimum MCSSC dose of  $100 \text{ mg}$  was sufficient for the removal of  $99.2\% \pm 0.4\%$ . However a maximum removal of  $65\% \pm 0.4\%$  of Cd(II) was observed for CSS with a dosage of  $300 \text{ mg}$ . It reveals that as the adsorbent dose increases, the number of active sites of the adsorbent also increases. After an optimum dose, a steady state is reached with an almost insignificant increase in Cd(II) removal, which may be due to the adsorption site aggregation or overlapping with the increase in adsorbent dose. Based on the adsorbent dose result indicates that MCSSC is 3 times more effective than that of CSS.

### 3.8. Effect of initial cadmium(II) ion concentration

The adsorption of Cd(II) ions from aqueous medium by CSS and MCSSC sorbent was studied from metal ion concentration of  $10\text{--}50 \text{ mg}\cdot\text{L}^{-1}$  at a  $\text{pH}$  6.0 and an optimum sorbent dose and contact time of  $300 \text{ mg}$ , 150 min for CSS and  $100 \text{ mg}$ , 120 min for MCSSC (Fig. 8). As the concentration of metal ions increases, the removal efficiency decreases from  $99.2\%$  to  $82.4\%$  for MCSSC and  $65.2\%$  to  $42.5\%$  for CSS. All metal ions surround the active regions at low concentrations, although some areas of the adsorbent surface are vacant. At higher concentrations, each site is coated by several metal ions, resulting in nearly constant adsorption capacity due to saturated points of adsorption. The accessible number of sites was maintained for the given dosage of adsorbent and adsorbing the equivalent amount of adsorbate, resulting in a decrease in removal efficiency. The more unfavourable absorption at higher concentrations is caused by an increase in the proportion of the initial number of moles to the accessible vacant sites.

3.9. Adsorption isotherms

The adsorption of cadmium(II) ions at equilibrium onto CSS and MCSSC were correlated by applying the non-linear forms of four different isotherm equations such as Freundlich, Langmuir, Temkin and Dubinin–Radushkevich at different temperatures (27°C–47°C) using MATLAB R2010b. According to the non-linear plot of  $q_e$  vs.  $C_e$  at various temperatures, the values for the isotherm parameters, root mean square error (RMSE), correlation coefficients ( $R^2$ ), and sum of squared error (SSE) for the removal of cadmium(II) ions onto CSS and MCSSC are listed in Table 1 and Fig. 9.

Comparative correlation coefficient  $R^2$ , SSE and RMSE values of Freundlich, Langmuir, Temkin and Dubinin–Radushkevich models indicate fitness of the adsorption data. However, higher value of correlation coefficient and lower value of SSE and RMSE of Langmuir model in comparison to other studied models is correlative of the monolayer distribution of Cd(II) ions on homogenous sites to the CSS and MCSSC surface. The  $R^2$  value is greater than 0.995 expressed that Langmuir isotherm favourable adsorption in the adsorption process. At 27°C, the Langmuir model demonstrates monolayer adsorption on homogenous active

sites of MCSSC and CSS with adsorption capacities of 540.85 and 27.65 mg·g<sup>-1</sup> of Cd(II) ions, respectively. According to the  $q_m$  values, MCSSC was approximately 19.6 times more efficient than CSS.

The Langmuir isotherm's  $R_L$  (Table 1) values fall in the range from 0 to 1, suggesting that cadmium(II) ions onto CSS and MCSSC indicating that the adsorption process is favourable. From this study, the uptake of cadmium(II) ions onto CSS and MCSSC from an aqueous solution is decreased with increasing temperature indicating that the adsorption process is exothermic.

The evaluation of the maximal monolayer adsorption rates of cadmium(II) ions onto different adsorbents using the Langmuir equation based on the literature survey are listed in Table 2. In the present study the value of cadmium(II) ions adsorption capacities are good agreement with other researcher values.

3.10. Thermodynamic studies

The effect of temperature was investigated for an adsorbent dose of 100 mg for MCSSC and 300 mg for CSS were

Table 1  
Non-linear isotherm and thermodynamic parameters for removal of Cd(II) ions

Isotherm methods	Parameters	Temperature					
		CSS		MCSSC		MCSSC	
		47°C	37°C	27°C	47°C	37°C	27°C
Dubinin–Radushkevich	$q_{mD}$ (mg·g <sup>-1</sup> )	14.22	18.66	20.87	25.78	29.15	34.54
	$E$ (kJ·mol <sup>-1</sup> )	1.190	1.123	1.111	1.724	1.887	1.923
	$\beta \times 10^{-7}$	3.536	3.979	4.665	1.688	1.412	1.354
	$R^2$	0.694	0.710	0.845	0.764	0.756	0.811
	RMSE	0.889	0.786	0.967	0.987	0.724	0.566
	SSE	12.39	15.43	16.38	35.65	29.54	24.65
	$A$ (L·mg <sup>-1</sup> )	1.054	1.124	1.267	1.987	2.075	2.354
Temkin	$b$ (kJ·mol <sup>-1</sup> )	1.495	1.317	1.031	1.143	1.047	0.944
	$B$	1.780	1.965	2.420	2.327	2.462	2.642
	$R^2$	0.934	0.927	0.945	0.938	0.945	0.924
	RMSE	0.987	0.741	0.675	0.965	0.864	0.879
	SSE	5.568	4.756	4.556	11.57	12.64	11.89
	$q_m$ (mg·g <sup>-1</sup> )	17.25	22.35	27.65	464.25	501.46	540.85
	$b$ (L·mg <sup>-1</sup> )	0.090	0.104	0.126	0.162	0.179	0.198
Langmuir	$R^2$	0.996	0.997	0.998	0.998	0.998	0.996
	RMSE	0.915	0.894	0.785	0.558	0.678	0.798
	SSE	2.021	2.012	1.136	13.08	3.279	1.056
	$R_L$	0.526–0.156	0.490–0.138	0.442–0.116	0.381–0.093	0.358–0.085	0.335–0.077
	$K_F$ (mg·g <sup>-1</sup> )	2.652	3.925	4.022	6.450	8.497	9.934
	$n$ (g·L <sup>-1</sup> )	1.827	1.615	1.782	1.827	1.756	1.925
	$R^2$	0.945	0.957	0.936	0.943	0.935	0.951
Freundlich	RMSE	0.992	0.789	1.034	0.698	0.856	0.755
	SSE	4.012	3.954	3.164	10.18	9.287	11.56
	$\Delta G^\circ$ (kJ·mol <sup>-1</sup> )	-4.616	-6.668	-11.461	-0.213	-0.727	-1.544
	$\Delta S^\circ$ (kJ·mol <sup>-1</sup> ·K <sup>-1</sup> )	-0.068			-0.337		
Thermodynamic	$\Delta H^\circ$ (kJ·mol <sup>-1</sup> )	-21.882			-112.114		

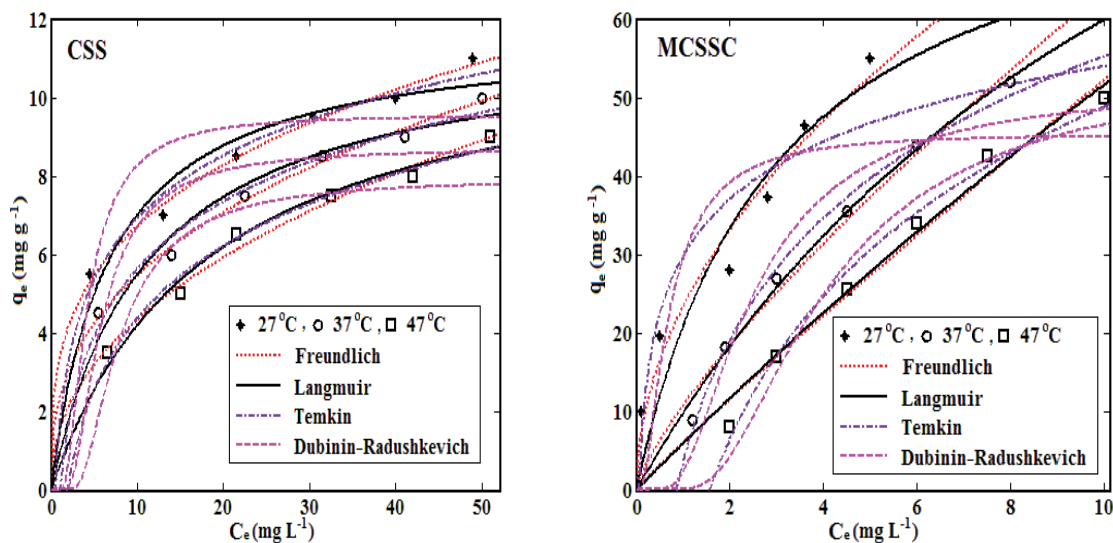


Fig. 9. Non-linear adsorption isotherm model for the removal of Cd(II) ions onto CSS and MCSSC.

Table 2

Comparison of Langmuir adsorption capacities on the removal of Cd(II) ions with other adsorbents

Adsorbents	Langmuir adsorption capacity ( $q_m$ , $\text{mg}\cdot\text{g}^{-1}$ )	References
Oyster shell	69.10	[10]
Palm oil shell	104.07	[11]
Palm kernel shell	38.00	[35]
Prawn shell	256.0	[36]
Cocoa pod husk	2.421	[9]
Walnut shell-rice husk	168.24	[37]
<i>Trapa natans</i> husk	33.90	[38]
Sunflower seed husks	81.97	[39]
Prickly pear seed cake	170.20	[7]
Mango peel	52.87	[8]
<i>Acacia senegal</i> pods	98.76	[40]
Neem ( <i>Azadirachta indica</i> ) leaf	154.50	[41]
<i>Eucalyptus camaldulensis</i>	6.17	[42]
CSS	27.65	Present study
MCSSC	540.85	Present study

added to 100 mL of  $10 \text{ mg}\cdot\text{L}^{-1}$  of cadmium(II) solution at pH 6.0, and the impact of temperature around  $27^\circ\text{C}$ – $47^\circ\text{C}$ . The elimination of Cd(II) reduced from 99% to 87% (MCSSC) and 65 to 52 (CSS) as the temperature rises, as shown in Fig. 10a, showing that the reaction was exothermic in nature. This might be caused by internal bonds breaking at lower temperatures, which would lead to more active sites at the MCSSC surface. The  $\Delta S^\circ$  and  $\Delta H^\circ$  values estimated from the intercept and slope of a plot of  $\ln K_c$  vs.  $1/T$ , (Fig. 10b), respectively. The thermodynamic parameters are listed in Table 1. The negative estimation of  $\Delta G^\circ$ , as given in Table 1, has confirmed the viability and spontaneity of the adsorption mechanism. Because of the negative values of  $\Delta H^\circ$ , the adsorption process was exothermic, which could be attributed to a weak interaction between  $\text{Cd}^{2+}$  and MCSSC.

It was further noted from Table 1 that the negative estimates in  $\Delta S^\circ$  shows the haphazardness at the solid–liquid interface.

### 3.11. Kinetic adsorption studies

The kinetic parameters of CSS and MCSSC derived from the kinetic models are shown in Table 3. The pseudo-second-order equation shows a good correlation of the experimental data resulted with linearized form of  $R^2$  value of closer to 0.999. The pseudo-first-order equation had a poor correlation when compared to the pseudo-second-order equation. Hence, the pseudo-second-order model equation was accepted as a useful model for kinetic studies for the adsorption of cadmium(II) ions onto CSS and MCSSC.

As a result, it is possible that the rate-limiting step in this sorption system is regulated by chemical sorption involving valence forces through the sharing or exchange of electrons between the sorbent and the sorbate.

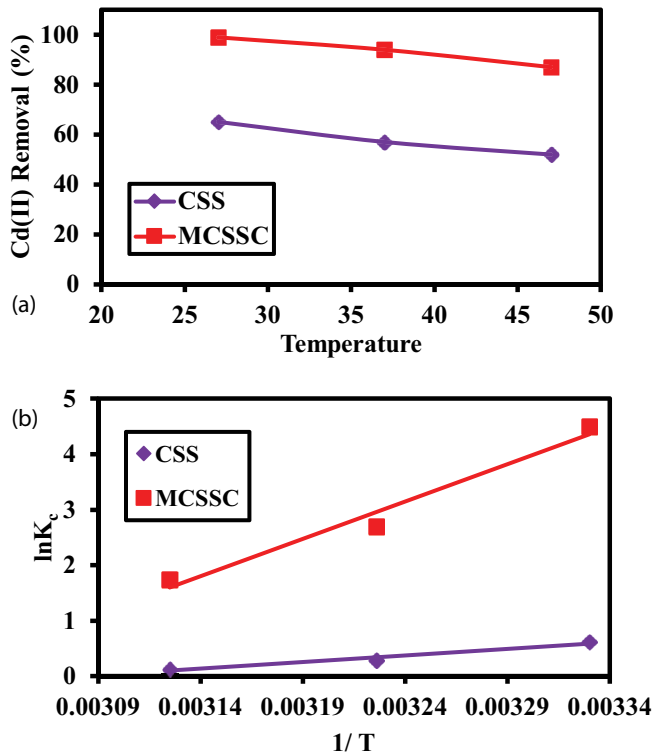


Fig. 10. (a) Effect of temperature on Cd(II) removal by CSS and MCSSC. (b) Thermodynamic diagrams for Cd(II) removal onto CSS and MCSSC.

In order to predict the rate controlling step the Weber and Morris [43] intraparticle diffusion model is a widely used to express the following equation:

$$q_t = k_d t^{1/2} + I \tag{16}$$

where the intraparticle diffusion rate constant is  $k_d$ , measured in  $\text{mg}\cdot\text{g}^{-1}\cdot\text{min}^{-1/2}$  and the constant  $I$  ( $\text{mg}\cdot\text{g}^{-1}$ ) estimates the boundary layer's thickness. It was shown that the boundary layer effect increased with increasing values of  $I$ . If the Weber–Morris plot of  $q_t$  vs.  $t^{1/2}$  results in a straight line, then intraparticle diffusion was the only mechanism controlling the sorption process, and the slope gives the value of rate constant,  $k_d$ . If the results showed that the multi-linear plots, this indicated that two or more steps influence the sorption process. According to Fig. 11a and b explored that the plots are diverted from their starting point at each concentration, and assumed that the rate-controlling factor not only the pore diffusion, but other factor, such as film diffusion, also played a role in the process of adsorption.

The following equation was used to estimate the pore and film diffusion coefficients, in order to identify the type of diffusion process that removes Cd(II) ions by CSS and MCSSC [44]:

$$D_p = 0.03r_o^2 t_{1/2} \tag{17}$$

$$D_f = \frac{0.23r_o \delta C^*}{C t_{1/2}} \tag{18}$$

where  $D_p$  and  $D_f$  represent the coefficient of pore and film diffusion ( $\text{cm}^2\cdot\text{s}^{-1}$ ),  $r_o$  denotes the sorbent radius (cm),  $\delta$  represents thickness of film (cm),  $t_{1/2}$  gives the value of half-life period (s) and  $C^*/C$  gives the loading of sorbent at

Table 3  
Kinetic constants for Cd(II) ion elimination on CSS and MCSSC

Kinetic model	Parameters	Concentrations ( $\text{mg}\cdot\text{L}^{-1}$ )					
		CSS			MCSSC		
		10	15	20	10	15	20
Pseudo-second-order	$q_{e,\text{exp}}$ ( $\text{mg}\cdot\text{g}^{-1}$ )	6.50	9.00	11.0	9.93	14.0	18.0
	$q_{e,\text{cal}}$ ( $\text{mg}\cdot\text{g}^{-1}$ )	6.49	8.63	10.8	10.2	13.9	18.3
	$k_2$ ( $\text{g}\cdot\text{mg}^{-1}\cdot\text{min}^{-1}$ )	0.010	0.014	0.010	0.008	0.017	0.006
	$R^2$	0.999	0.999	0.999	0.999	0.999	0.999
Pseudo-first-order	$q_{e,\text{cal}}$ ( $\text{mg}\cdot\text{g}^{-1}$ )	2.56	2.84	3.36	4.12	5.07	5.98
	$k_1$ ( $\text{min}^{-1}$ )	0.009	0.009	0.008	0.020	0.019	0.017
	$R^2$	0.954	0.948	0.961	0.962	0.975	0.967
Elovich model	$\beta$ ( $\text{g}^{-1}\cdot\text{mg}$ )	1.396	1.346	1.062	0.804	0.622	0.574
	$\alpha$ ( $\text{mg}\cdot\text{g}^{-1}\cdot\text{min}^{-1}$ )	14.57	263.3	234.6	22.55	58.94	251.9
	$R^2$	0.917	0.914	0.934	0.961	0.966	0.960
Intraparticle diffusion	$I$ ( $\text{mg}\cdot\text{g}^{-1}$ )	3.868	6.176	7.464	6.807	9.811	12.98
	$k_d$ ( $\text{mg}\cdot\text{g}^{-1}\cdot\text{min}^{-1/2}$ )	0.151	0.151	0.196	0.228	0.313	0.353
	$R^2$	0.948	0.932	0.950	0.916	0.916	0.921
Film diffusion	$D_f$ ( $\times 10^{-8} \text{ cm}^2\cdot\text{s}^{-1}$ )	0.716	1.389	1.212	0.876	2.622	1.190
Pore diffusion	$D_p$ ( $\times 10^{-8} \text{ cm}^2\cdot\text{s}^{-1}$ )	4.133	8.679	8.266	3.306	0.105	4.959

equilibrium. In the adsorption of heavy metal ions on the CSS and MCSSC surface (Table 3), if the coefficient of film diffusion values ( $D_f$ ) falls between  $10^{-6}$  and  $10^{-8}$   $\text{cm}^2\cdot\text{s}^{-1}$  then the rate determining process followed by mechanism of film diffusion. The pore diffusion coefficient ( $D_p$ ) should be between  $10^{-11}$ – $10^{-13}$   $\text{cm}^2\cdot\text{s}^{-1}$  then the rate-limiting component will be the pore diffusion.

According to Table 3, the values of the film diffusion coefficient for CSS and MCSSC were between  $10^{-6}$ – $10^{-8}$   $\text{cm}^2\cdot\text{s}^{-1}$ , showing that the adsorption of cadmium(II) was followed by a film diffusion process. Thus, it can be concluded from the Weber–Morris model and the film diffusion coefficients derived from the aforementioned studies that both film diffusion and intraparticle diffusion processes contribute to the removal of heavy metal ions.

### 3.12. Separation of solid–liquid

For the practical application of an adsorption system, the solid–liquid separation process is important. In a 100 mL

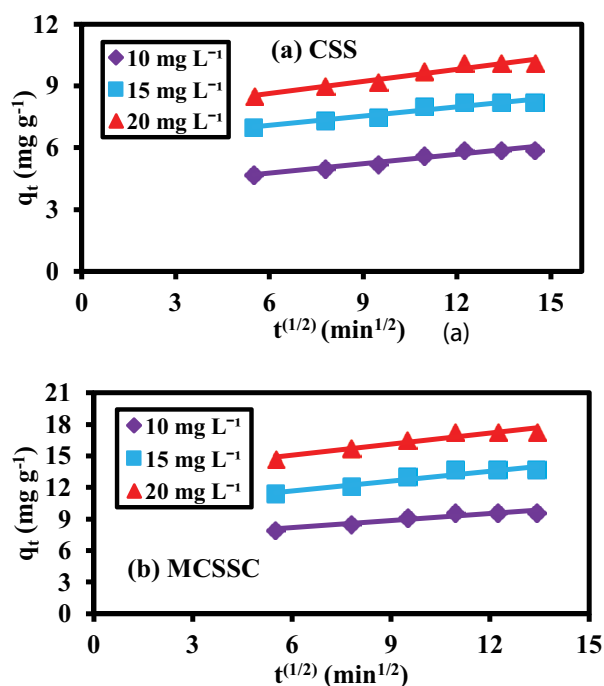


Fig. 11. (a,b) Plots of intraparticle diffusion for the elimination of Cd(II).

beaker, a precisely weighed 100 mg sample of MCSSC was dissolved in 10  $\text{mg}\cdot\text{L}^{-1}$  of cadmium(II) solution. The simplest method for separating solids from liquids is sedimentation. Fig. 12 shows how to separate bioadsorbents from homogenised MCSSC solutions both with and without the use of an external magnetic field. The time 2 min is needed for the final sedimentation of MCSSC to the bottom of the tubes in the absence of an external magnetic field. However, the time needed for complete separation of MCSSC was significantly shortened to within 20 s in the presence of an external magnetic field. This result strongly shows that the magnetic bioadsorbent based on  $\text{Fe}_3\text{O}_4$  coated castor seed shell can be removed from solutions more readily and quickly than untreated bioadsorbents under an external magnetic field. These findings are therefore extremely important for the further usage and treatment of used bioadsorbents.

### 4. Removal of Cd(II) from electroplating wastewater and regeneration studies

To demonstrate the usefulness of sorbents in batch mode investigations, batch experiments with cadmium(II) ions containing electroplating wastewater were conducted. The



Fig. 12. MCSSC particles in Cd(II) solution, before (a) and after (b) magnetic separation.

Table 4  
Removal efficiencies of MCSSC and CSS from cadmium-electroplating wastewater

Parameter	Before treatment ( $\text{mg}\cdot\text{L}^{-1}$ )	After treatment ( $\text{mg}\cdot\text{L}^{-1}$ ) remaining concentration		Removal (%)	
		MCSSC	CSS	MCSSC	CSS
Cadmium(II)	130.00	0.80	47.60	99.4	63.4
Chloride	750.00	110.00	400.00	85.33	46.67
Sulfate	870.00	130.00	600.00	84.81	85.06
Bicarbonate	140.00	35.00	95.00	75.00	32.14
Calcium	27.00	07.00	15.00	74.10	44.44

Table 5  
Five cycles of Cd(II) ion adsorption–desorption by CSS and MCSSC with 0.5 N HCl

Cycles	Cd(II) $C_0$ (mg·L <sup>-1</sup> )	CSS		MCSSC	
		Adsorption (%)	Recovery (%)	Adsorption (%)	Recovery (%)
1	130	63.40	59.45	99.40	99.34
2	130	58.37	56.41	99.17	99.25
3	130	53.50	50.57	99.22	99.15
4	130	48.24	43.35	99.10	99.32
5	130	38.78	28.14	99.20	99.13

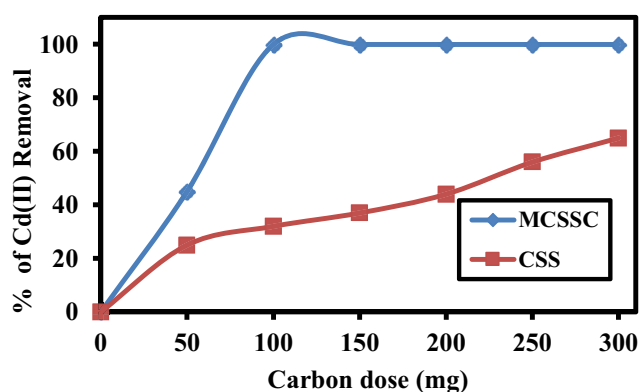


Fig. 13. Effectiveness of CSS and MCSSC dosage on Cd(II) ion adsorption from wastewater.

suitability of the prepared MCSSC and CSS was checked by collecting the wastewater sample from the nearby industrial area in Tirupur (Table 4). The experiments were conducted with 1 L wastewater solution containing 130 mg·L<sup>-1</sup> of Cd(II) solutions adjusted at an optimum pH and in the presence of varying amount of adsorbent doses under respective optimum period of 120 min for MCSSC and 150 min for CSS. It is clear that from Fig. 13, the 99.3% of Cd(II) ions were eliminated at a minimal MCSSC dosage of 1 g·L<sup>-1</sup>. On the other hand of CSS, an adsorbent dose of 3.0 g·L<sup>-1</sup> might be sufficient to remove the maximum amounts of 64.5 ± 0.4. According to the aforementioned results, MCSSC is three times more efficient than CSS.

The 0.5 N HCl was employed as the regenerating agent for five cycles of batch mode operation to test the adsorbent's stability for repeated uses. The recyclability studies demonstrated that the recycled MCSSC behaves like a fresh adsorbent for the removal of cadmium(II) ions even after five cycles (Table 5). It was discovered that both adsorption and desorption significantly decreased in the case of CSS (Table 5). As a result, it is important to note that the MCSSC can be reused for at least 5 cycles by the removal of heavy metal ions from wastewater.

## 5. Conclusions

The present investigation shows that the castor seed shell, in their native (CSS) and modified with Fe<sub>3</sub>O<sub>4</sub> loaded activated carbon (MCSSC), can be utilized as an effective adsorbent for the treatment of wastewater containing Cd(II) ions.

The maximum percentage of cadmium(II) elimination was achieved in 120 and 150 min for MCSSC and CSS, beyond which there was no significant change. The results revealed that the effectiveness of removal is significantly pH dependant, with 99.2% ± 0.4% (MCSSC) and 47% ± 0.4% (CSS) Cd(II) removal at 6.0. The maximum Cd(II) ion removal onto MCSSC was observed at an adsorbent dose of 100 mg. On the other hand, CSS was found to be with an adsorbent dose of 300 mg. The FTIR spectra revealed that the presence of various functional groups, including hydroxyl, carboxylic, and Fe–O groups are responsible for the adsorption of metal ions by MCSSC. The surface morphology and elemental analysis of the MCSSC and CSS was examined using SEM, TEM images and EDX spectrum. The maximum Cd(II) uptake capacities onto MCSSC was at 540.85 mg·g<sup>-1</sup> but in case of CSS was about 27.65 mg·g<sup>-1</sup>. Measurements of thermodynamics confirmed the exothermic and spontaneous character of the adsorption process. The pseudo-second-order model provided the most accurate description of the adsorption kinetics and the rate controlling step is the film diffusion process. When compared to CSS, the MCSSC has a great potential for removing Cd(II) ions from industrial effluent and can be reused five times without decreasing efficiency. As a result, magnetic nanocomposite loaded castor seed shell carbon was demonstrated to be an efficient removal of heavy metal ions with good recovery and regeneration capabilities.

## References

- [1] Y.C. Sharma, Thermodynamics of removal of cadmium by adsorption on indigenous clay, *Chem. Eng. J.*, 145 (2008) 64–68.
- [2] S. Sribharathi, P. Anitha, R. Sudha, K. Poornima, G. Kavitha, Cadmium(II) removal from aqueous solution using a novel magnetic nanoparticle impregnated onto *Citrus hystrix* leaves, *Desal. Water Treat.*, 196 (2020) 388–401.
- [3] L. Sun, P. Gong, Y. Sun, Q. Qin, K. Song, J. Ye, H. Zhang, B. Zhou, Y. Xue, Modified chicken manure biochar enhanced the adsorption for Cd<sup>2+</sup> in aqueous and immobilization of Cd in contaminated agricultural soil, *Sci. Total Environ.*, 851 (2022) 158252, doi: 10.1016/j.scitotenv.2022.158252.
- [4] WHO, World Health Organization Guidelines for Drinking Water Quality, Recommendations, World Health Organisation, Geneva, 2008.
- [5] H. Gong, J. Chi, Z. Ding, F. Zhang, J. Huang, Removal of lead from two polluted soils by magnetic wheat straw biochars, *Ecotoxicol. Environ. Saf.*, 205 (2020) 111132, doi: 10.1016/j.ecoenv.2020.111132.
- [6] R. Sudha, P. Premkumar, Comparative studies on the removal of chromium(VI) from aqueous solutions using raw and modified *Citrus limettoides* peel, *Indian J. Chem. Technol.*, 25 (2018) 255–265.

- [7] R. Dhahri, M. Yilmaz, L. Mechi, A.K.D. Alsukaibi, F. Alimi, R. Salem, Y. Moussaoui, Optimization of the preparation of activated carbon from prickly pear seed cake for the removal of lead and cadmium ions from aqueous solution, *Sustainability*, 14 (2022) 3245, doi: 10.3390/su14063245.
- [8] I.K. Rind, N. Memon, M.Y. Khuhawar, W.A. Soomro, M.F. Lanjwani, Modeling of cadmium(II) removal in a fixed bed column utilizing hydrochar-derived activated carbon obtained from discarded mango peels, *Sci. Rep.*, 12 (2022) 8001, doi: 10.1038/s41598-022-11574-1.
- [9] A.F. Adeyemi, L.O. Olasunkanmi, Evaluation of the efficiency of ZnCl<sub>2</sub> activated cocoa pod husk charcoal on the removal of Cu<sup>2+</sup>, Cd<sup>2+</sup>, and Pb<sup>2+</sup> ions from aqueous solution, *J. Dispersion Sci. Technol.*, 44 (2021) 1900–1909.
- [10] S. Wu, L. Liang, Q. Zhang, L. Xiong, S. Shi, Z. Chen, Z. Lu, L. Fan, The ion-imprinted oyster shell material for targeted removal of Cd(II) from aqueous solution, *J. Environ. Manage.*, 302 (2022) 114031, doi: 10.1016/j.jenvman.2021.114031.
- [11] Buhani, Suharso, M. Rilyanti, M. Sari, Sumadi, Removal of Cd(II) ions in solution by activated carbon from palm oil shells modified with magnetite, *Desal. Water Treat.*, 218 (2021) 352–362.
- [12] Y. Yan, F. Qi, L. Zhang, P. Zhang, Q. Li, Enhanced Cd adsorption by red mud modified bean-worm skin biochars in weakly alkali environment, *Sep. Purif. Technol.*, 297 (2022) 121533, doi: 10.1016/j.seppur.2022.121533.
- [13] Q. Su, S. Li, M. Chen, X. Cui, Highly efficient Cd(II) removal using macromolecular dithiocarbamate/slag-based geopolymer composite microspheres (SGM-MDTC), *Sep. Purif. Technol.*, 286 (2022) 120395, doi: 10.1016/j.seppur.2021.120395.
- [14] W. Zhao, K. Feng, H. Zhang, L. Han, Q. He, F. Huang, W. Yu, F. Guo, W. Wang, Sustainable green conversion of coal gangue waste into cost-effective porous multimetallic silicate adsorbent enables superefficient removal of Cd(II) and dye, *Chemosphere*, 324 (2023) 138287, doi: 10.1016/j.chemosphere.2023.138287.
- [15] C. Hong, Z. Dong, J. Zhang, L. Zhu, L. Che, F. Mao, Y. Qiu, Effectiveness and mechanism for the simultaneous adsorption of Pb(II), Cd(II) and As(III) by animal-derived biochar/ferrihydrite composite, *Chemosphere*, 293 (2022) 133583, doi: 10.1016/j.chemosphere.2022.133583.
- [16] M. Hassan, R. Naidu, J. Du, F. Qi, M.A. Ahsan, Y. Liu, Magnetic responsive mesoporous alginate/β-cyclodextrin polymer beads enhance selectivity and adsorption of heavy metal ions, *Int. J. Biol. Macromol.*, 207 (2022) 826–840.
- [17] H.M.F. Freundlich, Over the adsorption in solution, *J. Phys. Chem.*, 57 (1906) 385–470.
- [18] I. Yousaf, U. Rahman, K. Mansoor, Solid phase extraction of Pb(II) and Cd(II) using reduced graphene oxide-polychloroprene impregnated with magnetic nanoparticle (MNP<sub>s</sub>-RGO-PCP), *Desal. Water Treat.*, 114 (2018) 232–241.
- [19] M.J. Temkin, V. Pyzhev, Recent modifications to Langmuir isotherms, *Acta Phys.-URSS*, 12 (1940) 217–225.
- [20] M.M. Dubinin, L.V. Radushkevich, Equation of the characteristic curve of activated charcoal, *Chem. Zent.*, 1 (1947) 875–889.
- [21] S. Bhattacharjee, S. Chakrabarty, S. Maity, S. Kar, P. Thakur, G. Bhattacharaya, Removal of lead from contaminated water bodies using sea nodule as an adsorbent, *Water Res.*, 55 (2003) 327–329.
- [22] O. Celebi, C. Uzum, T. Shahwan, H.N. Erten, A radiotracer study of the adsorption behaviour of aqueous Ba<sup>2+</sup> ions on nanoparticles of zero-valent iron, *J. Hazard. Mater.*, 148 (2007) 761–767.
- [23] P. Senthil Kumar, M. Palaniyappan, M. Priyadharshini, A.M. Vignesh, A. Thanjiappan, S.A. Fernando, R. Tanvir Ahmed, R. Srinath, Adsorption of basic dye onto raw and surface – modified agricultural waste, *Environ. Prog. Sustainable Energy*, 33 (2014) 87–98.
- [24] S. Sun, J. Yang, Y. Li, K. Wang, X. Li, Optimizing adsorption of Pb(II) by modified litchi pericarp using the response surface methodology, *Ecotoxicol. Environ. Saf.*, 108 (2014) 29–35.
- [25] M. Avila, T. Burks, F. Akhtar, M. Göthelid, P.C. Lansäker, M.S. Toprak, M. Muhammed, A. Uheida, Surface functionalized nanofibers for the removal of chromium(VI) from aqueous solutions, *Chem. Eng. J.*, 245 (2014) 201–209.
- [26] M. Khan, E. Yilmaz, B. Sevinc, E. Sahmetlioglu, J. Shah, M.R. Jan, M. Soylak, Preparation and characterization of magnetic allylamine modified graphene oxide-poly(vinyl acetate-co-divinylbenzene) nanocomposite for vortex assisted magnetic solid phase extraction of some metal ions, *Talanta*, 146 (2016) 130–137.
- [27] N.T. Abdel-Ghani, G.A. El-Chaghaby, Biosorption for metal ions removal from aqueous solutions: a review of recent studies, *Int. J. Latest Res. Sci. Technol.*, 3 (2014) 24–42.
- [28] A.S. Thajeel, Modeling and optimization of adsorption of heavy metal ions onto local activated carbon, *Aquat. Sci. Technol.*, 1 (2013) 108–134.
- [29] G.Y. Li, Y.R. Jiang, K.L. Huang, P. Ding, J. Chen, Preparation and properties of magnetic Fe<sub>3</sub>O<sub>4</sub>-chitosan nanoparticles, *J. Alloys Compd.*, 466 (2008) 451–456.
- [30] R. Sharma, A. Sarswat, C.U. Pittman, D. Mohan, Cadmium and lead remediation using magnetic and non-magnetic sustainable biosorbents derived from *Bauhinia purpurea* pods, *RSC Adv.*, 7 (2017) 8606–8624.
- [31] R.G. Poonam, S.K. Bharti, N. Kumar, Kinetic study of lead (Pb<sup>2+</sup>) removal from battery manufacturing wastewater using bagasse biochar as biosorbent, *Appl. Water Sci.*, 8 (2018) 1–13.
- [32] A.A. Guilherme, P.V.F. Dantas, E.S. Santos, F.A.N. Fernandes, G.R. Macedo, Evaluation of composition, characterization and enzymatic hydrolysis of pretreated sugar cane bagasse, *Braz. J. Chem. Eng.*, 32 (2015) 23–33.
- [33] W. Kong, J. Ren, S. Wang, Q. Chen, Removal of heavy metals from aqueous solutions using acrylic-modified sugarcane bagasse-based adsorbents: equilibrium and kinetics studies, *BioResources*, 9 (2014) 3184–3196.
- [34] M. Kadari, M. Makhlof, O. Ould Khaoua, M. Kesraoui, S. Bouriche, Z. Benmaamar, The removal efficiency of cadmium (Cd<sup>2+</sup>) and lead (Pb<sup>2+</sup>) from aqueous solution by graphene oxide (GO) and magnetic graphene oxide (α-Fe<sub>2</sub>O<sub>3</sub>/GO), *Chem. Afr.*, 6 (2023) 1515–1528.
- [35] R. Baby, M.Z. Hussein, Z. Zainal, A.H. Abdullah, Functionalized activated carbon derived from palm kernel shells for the treatment of simulated heavy metal-contaminated water, *Nanomaterials (Basel)*, 11 (2021) 3133, doi: 10.3390/nano11113133.
- [36] J. Guo, Y. Song, X. Ji, L. Ji, L. Cai, Y. Wang, H. Zhang, W. Song, Preparation and characterization of nanoporous activated carbon derived from prawn shell and its application for removal of heavy metal ions, *Materials (Basel)*, 12 (2019) 241, doi: 10.3390/ma12020241.
- [37] L.T. Popoola, Nano-magnetic walnut shell-rice husk for Cd(II) sorption: design and optimization using artificial intelligence and design expert, *Heliyon*, 5 (2019) e02381, doi: 10.1016/j.heliyon.2019.e02381.
- [38] W. Yin, C. Zhao, J. Xu, J. Zhang, Z. Guo, Y. Shao, Removal of Cd(II) and Ni(II) from aqueous solutions using activated carbon developed from powder-hydrolyzed-feathers and *Trapa natans* husks, *Colloids Surf., A*, 560 (2019) 426–433.
- [39] W. Srisuwan, C. Jubsilp, S. Srisorrachatr, The use of K<sub>2</sub>CO<sub>3</sub> modified sunflower seed husks for removing of metal ions from industrial wastewater, *Chem. Eng. Trans.*, 70 (2018) 241–246.
- [40] A.A. Adetokun, S. Uba, Z.N. Garba, Optimization of adsorption of metal ions from a ternary aqueous solution with activated carbon from *Acacia senegal* (L.) Willd pods using central composite design, *J. King Saud Univ.-Sci.*, 31 (2019) 1452–1462.
- [41] H. Patel, Batch and continuous fixed bed adsorption of heavy metals removal using activated charcoal from neem (*Azadirachta indica*) leaf powder, *Sci. Rep.*, 10 (2020) 16895, doi: 10.1038/s41598-020-72583-6.
- [42] H. Gebretsadik, A. Gebrekidan, L. Demlie, L.N. Suvarapu, Removal of heavy metals from aqueous solutions using *Eucalyptus camaldulensis*: An alternate low cost adsorbent, *Cogent Chem.*, 6 (2020) 1720892, doi: 10.1080/23312009.2020.1720892.
- [43] W.J. Weber, J.C. Morris, Kinetics of adsorption on carbon from solution, *J. Sanit. Eng. Div. Am. Soc. Civ. Eng.*, 89 (1963) 31–60.
- [44] A.K. Bhattacharya, C.J. Venkobachar, Removal of cadmium(II) by low cost adsorbents, *J. Environ. Eng. Div.-ASCE*, 110 (1984) 110–122.